A Minkowski space embedding to understand Markov models dynamics

David Andrieux

To describe the behavior of Markov models as parameters are varied, I show how to embed the space of Markov models within a Minkowski space. This embedding maintains the inherent distance between different instances of the model. The coordinates of this embedding emerge from the symmetrized Kullback-Leibler divergence and are expressed in terms of thermodynamic quantities, organizing the Minkowski space into equilibrium and nonequilibrium components. With this approach, we can visualize models' behaviors and gain a thermodynamic interpretation of information geometric concepts, even in far-from-equilibrium scenarios. I illustrate this approach using an analytically solvable molecular motor model.

CONTEXT AND OBJECTIVES

To gain insight into a system's dynamical and thermodynamical properties, it is crucial to understand their variations across the parameter space. For Markov models, however, the space of parameters has no obvious intrinsic structure. For example, multiple combinations of parameters can lead to the same affinities and currents, creating ambiguity and arbitrariness in their nonequilibrium response [1, 2]. Analysis of parameter sensitivity also shows that most models are 'sloppy', in the sense that they have a hierarchy of eigenvalues spanning multiple scales [3, 4].

One approach to tackle these challenges is through the lens of stochastic thermodynamics. In stochastic thermodynamics, the (thermo)dynamical properties of the system are examined as parameters are varied [5, 6]. In the linear regime, the parameter space has a natural structure based on the Fisher information metric, which is linked to equilibrium fluctuations [7, 8]. Outside the linear regime, however, the structure of the parameter space and its connections to thermodynamics has remained largely unexplored. One notable exception are dynamical equivalence classes, which provide a 'hidden' structure in the parameter space induced by their transport properties [9]. These equivalence classes uniquely characterize the nonequilibrium conditions and parameters of the system, providing a well-defined and symmetric nonequilibrium theory [10].

Another important angle to study the space of parameters is through the lens of information geometry. In information geometry, the space of parameters (e.g., for probability distributions or Markov dynamics) is analyzed by introducing a divergence as a measure of the separation between models [11, 12]. In this context, Teoh et al. demonstrated that the symmetrized Kullback-Leibler divergence plays a special role in vizualizing probabilistic models [13, 14]. The symmetrized KL divergence induces a Minkowksi structure in the space of probabilistic models which preserves the 'distance' between models.

This paper brings these different concepts and results together. Following the approach of Teoh et al. [14], I show that the space of Markov models possesses a Minkoswki structure induced by the symmetrized Kullback-Leibler divergence. In this Minkowski space, the embedding coordinates disantangle the system's equilibrium and nonequilibrium components. The former is expressed in terms of kinetic activities and forces while the latter coincides with the dynamical equivalence classes and are expressed in terms of thermodynamic currents and affinities [6]. These findings provide a unified and systematic way to study nonequilibrium Markov systems and their dynamical properties.

I. THERMODYNAMIC DECOMPOSITION OF THE SPACE OF MARKOV CHAINS

Let's consider the space Λ of primitive Markov chains on a finite state space of size N. A Markov chain $P \in \Lambda$ admits a unique stationary state π and can be depicted as a graph with N states, S self-transitions, and E edges, each edge representing the allowed transition between states.

The space Λ has $M = 2E + S - N$ dimensions while the subspace Σ of equilibrium systems has dimension $E + S - 1$. A chain P then has $E - N + 1$ independent currents J_α and affinities A_α [1, 15]. Each independent current is associated with a fundamental cycle in the graph and a specific edge α [1, 15].

Multiple representations of the spaces Λ and Σ exist, e.g. using exponential families [11, 12, 16] or the rotational representation of Markov chains [17, 18]. Here I will represent the space Λ using a thermodynamic decomposition [9]. In this decomposition, a chain P is determined by an equilibrium component E and by it affinities A_α as

$$P = s\left[E \circ Z(\boldsymbol{A})\right] . \tag{1}$$

Here the mapping s transforms a positive matrix into a stochastic one:

$$s[K] = \frac{1}{\rho}\mathrm{diag}(\beta)^{-1} K \, \mathrm{diag}(\beta) ,$$

where ρ is the largest eigenvalue of K and β its largest right eigenvector. The matrix

$$Z_{ij} \equiv \begin{cases} \exp\left(\pm A_\alpha/2\right) & \text{if } i \to j = \alpha \text{ in the } \pm \text{ direction,} \\ 1 & \text{otherwise} \end{cases}$$

captures the nonequilibrium (asymmetric) components of P. The equilibrium component E of a given P can be recovered as $E = s[(P \circ P^T)^{(1/2)}]$, where $P^{(1/2)}$ denotes the Hadamard or elementwise exponentiation (E is often denoted by $P^{(e)}$ in information geometry). The full space of Markov models is then obtained by varying the elements $E \in \Sigma$ and the affinities A_α.

The dynamics P sharing the same equilibrium component E in the decomposition (1) are expected to display similar properties [9]. These *dynamical equivalence classes* indeed play a special role in nonequilibrium transport [20]. For example, the equilibrium and nonequilibrium fluctuations are identical within an equivalence class [19]. In addition, the currents fluctuations can be obtained from the current response curve itself and all response coefficients are fully symmetric and are expressed in terms of equilibrium coefficients [10]. The equivalence classes also capture the minimal distance, in the information-theoretic sense, between models under fixed nonequilibrium conditions [2].

The decomposition (1) offers a clear thermodynamic interpretation and provides important features when studying transport properties [10, 19]. However, it still lacks a natural geometric structure or notion of distance. In the next section, I show how the space Λ can be embedded in a Minkowski space with a clear physical interpretation.

II. INTENSIVE EMBEDDING IN MINKOWSKI SPACE

Teoh et al. showed that the symmetrized Kullback-Leibler divergence D_{sKL} offers a natural distance in the space of exponential families of probability distributions [14]. Using that distance [21], an exponential family of probability distributions f with N parameters can be embedded isometrically in a $N + N$-dimensional Minkowski space. That is, D_{sKL} can be decomposed into $N + N$ components $S_i^\pm(f)$ such that

$$D_{sKL}(f, f') = \sum_{i=1}^{N} \left[\left(\Delta S_i^+\right)^2 - \left(\Delta S_i^-\right)^2 \right],$$

with $\Delta S_i^\pm = S_i^\pm(f) - S_i^\pm(f')$. Using these $N + N$ coordinates, the models can be visualized as control parameters are varied, preserving the distance between probability distributions. All pairwise distances between model instances are given by the symmetrized Kullback-Leibler divergence [14].

In this section I adapt this approach to the context of Markov chains and show that the resulting coordinates have a clear physical interpretation in terms of kinetic and thermodynamical quantities.

The symmetrized Kullback-Leibler divergence between two Markov chains reads

$$
\begin{aligned}
D_{sKL}(P||G) &= D_{KL}(P||G) + D_{KL}(G||P) \\
&= \sum_{ij} [\pi_i P_{ij} - \nu_i G_{ij}] \ln \frac{P_{ij}}{G_{ij}} \geq 0 . \quad (2)
\end{aligned}
$$

Here $D_{KL}(P||G) = \sum_{ij} \pi_i P_{ij} \ln P_{ij}/G_{ij}$ is the Kullback-Leibler divergence and π and ν are the stationary distributions of P and G, respectively.

To calculate and recast the divergence (2) in a more useful form, I now use the thermodynamic decomposition $P = s[E \circ Z]$ and $G = s[E' \circ Z']$. As demonstrated in appendix A, this leads to

$$
\begin{aligned}
D_{sKL}(P||G) &= \frac{1}{2} \sum_{\alpha} (A_\alpha - A_\alpha')(J_\alpha - J_\alpha') \\
&+ \frac{1}{2} \sum_{e} (X_e - X_e')(Y_e - Y_e') . \quad (3)
\end{aligned}
$$

Here J_α is the average current with corresponding affinity A_α while $Y_e = \pi_i P_{ij} + \pi_j P_{ji}$ is the activity along the edge $e = i \longleftrightarrow j$ and $X_e = \ln P_{ij} P_{ji}$. By analogy with the affinities, the quantities X_e play the role of 'kinetic forces' driving the activity Y_e along the edge [22].

Not all variables Y_e, however, are independent since $\sum_e Y_e = 1$. One variable r can thus be eliminated as $Y_r = 1 - \sum_{e \neq r} Y_e$. With this substitution, Eq. (3) retains the same form but with effective forces

$$\bar{X}_e = X_e - X_r .$$

For notational simplicity, in the rest of the paper I assume that one of the dependent edge e has been eliminated and write $X_e = \bar{X}_e$.

The divergence (3) between two models P and G comprises two types of contributions. The first contribution captures the nonequilibrium (or antisymmetric) aspects and is expressed in terms of the thermodynamic current and affinities, while the second contribution reflects the changes in the equilibrium (or symmetric) part of the dynamics. As I will argue below, the divergence (3) measures both the time and 'spatial' asymmetry between two models.

Let's now express the divergence (3) in terms of space-time coordinates. As shown in appendix A, the coordinates

$$S_\alpha^\pm = \frac{1}{4}(A_\alpha \pm J_\alpha) \quad \text{and} \quad S_e^\pm = \frac{1}{4}(X_e \pm Y_e) \quad (4)$$

provide an intensive embedding in a $M + M$ Minkowski space:

$$D_{sKL}(P||G) = \sum_{l=1}^{M} \left[(\Delta S_l^+)^2 - (\Delta S_l^-)^2 \right] \geq 0 , \quad (5)$$

where the sum runs over $l = (\alpha, e)$ with $e \neq r$.

The Minkowski space is $M + M$ dimensional, where $M = 2E + S - N$ corresponds to the number of independent parameters of the Markov models. The spacelike coordinates S^+ are greater than the timelike coordinates S^- for each variable, $[S_l^+(P) - S_l^+(G)]^2 \geq [S_l^-(P) - S_l^-(G)]^2$. It is also possible to center and rescale the coordinates by factors λ_l, e.g. to minimize the sum of the square of the coordinates or adjust the units [14].

Using coordinates (4), the set of Markov chains can thus be vizualized as a manifold as control parameters are varied, preserving the symmetric divergence between systems and with clear thermodynamic interpretation of the coordinates. This constitues our main result.

III. KINETIC AND THERMODYNAMICS PROPERTIES OF THE MODEL MANIFOLD

I now explore the kinetic and thermodynamic properties of the embedding (5) before analyzing an example of molecular motor in Section IV. Taken together, the results below show that the symmetrized KL divergence measures both the time asymmetry (through the currents and affinities) and the spatial asymmetry (through the activities and kinetic forces) of the dynamics.

A. Equilibrium and iso-affinity manifolds

Let's first consider the case where the affinities between models are identical, $A_\alpha = A'_\alpha$. In these sub-manifolds, the separations $\Delta S_\alpha^\pm$ vanish and the divergence (3) simplifies to

$$D_{sKL}(P||G) = \sum_e \left[(\Delta S_e^+)^2 - (\Delta S_e^-)^2 \right]$$
$$= \frac{1}{2} \sum_e (X_e - X'_e)(Y_e - Y'_e).$$

The embedding coordinates and the separation between two models are directly expressed in terms of the systems' activities and kinetic forces X_e and X'_e, which in turn measure the inhomogeneity (spatial asymmetry) of the dynamics across the graph.

Note, however, that the coordinates $S_\alpha^\pm$ still vary along the iso-affinity manifold even if $\Delta S_\alpha^\pm = 0$. Only when $A_\alpha = 0$ are the coordinates $S_\alpha^\pm$ independent of $S_e^\pm$ (more precisely, $S_\alpha^\pm = 0$ in that case). The equilibrium manifold is thus special in the sense that it is entirely described by the coordinates $S_e^\pm$.

B. Dynamical equivalence classes

Dynamical equivalence classes play a special role in nonequilibrium response theory [10]. Remarkably, they emerge naturally in this framework.

A dynamical equivalence class is obtained when all the model instances share the same equilibrium component E, i.e. when $X_e = X'_e$. In that case the separations $\Delta S_e^\pm$ vanish and the symmetrized KL divergence (3) simplifies to

$$D_{sKL}(P||G) = \sum_\alpha \left[(\Delta S_\alpha^+)^2 - (\Delta S_\alpha^-)^2 \right]$$
$$= \frac{1}{2} \sum_\alpha (A_\alpha - A'_\alpha)(J_\alpha - J'_\alpha).$$

The embedding coordinates and the separation between two models in an equivalence class are directly expressed in terms of the system's thermodyamic currents and affinities, which in turn measure the time asymmetry of the dynamics.

As in the case of the iso-affinity manifolds, the coordinates $S_e^\pm$ vary along the dynamical equivalence class even if $\Delta S_e^\pm = 0$. In contrast to the equilibrium case however, even when $X_e = 0$ the coordinates $S_e^\pm = \pm Y_e$ still depend on $S_\alpha^\pm$. Nonetheless, the class $X_e = 0$ can act as a distinct reference dynamics: it is obtained from $E = s[T]$, where T is the adjacency matrix of P, and thus corresponds to Markov models derived from a 'spatially homogeneous' equilibrium component (this will be illustrated in the molecular motor example in section IV).

C. Entropy production

The dissipation or entropy production $\Delta_i S = \sum_\alpha J_\alpha A_\alpha \geq 0$ plays an important role in thermodynamics. In the present framework, the entropy production emerges as the symmetrized KL divergence with respect to the equilibrium component $E = P^{(e)}$ [23]:

$$\Delta_i S = \sum_\alpha J_\alpha \times A_\alpha = 2 D_{sKL}(P||E)$$

since $J'_\alpha = A'_\alpha = 0$ and $X'_e = X_e$ as E belong to the equivalence class of P.

The entropy production can also be obtained as $D_{sKL}(P||P^{(m)})$ where $P^{(m)} = (P + P^*)/2$ with P^* the time-reversed dynamics [23]. This occurs because $J'_\alpha = A'_\alpha = 0$ and $Y'_e = Y_e$ in that case.

Finally, the entropy production can also be expressed as the divergence between a dynamics and its time-reserval [23, 24]: $\Delta_i S = 2 D_{sKL}(P||P^*)$, as seen from Eq. (3) and using that the currents and affinities of P^* take opposite values compared to P while having the same equilibrium components [25].

IV. A MOLECULAR MOTOR EXAMPLE

Consider a Markov chain representing a molecular motor with 2ℓ states corresponding to different conformations of the protein complex. These states form a cycle

of periodicity 2ℓ corresponding to a revolution by 360° for a rotary motor or a reinitialization step for a linear motor. The motor alternates between two types of states according to the transition matrix [26]

$$P = \begin{pmatrix} 0 & p_1 & & & & & 1-p_1 \\ 1-p_2 & & p_2 & & & & \\ & 1-p_1 & & p_1 & & & \\ & & \ddots & 0 & \ddots & & \\ & & & 1-p_1 & 0 & p_1 & \\ p_2 & & & & 1-p_2 & 0 & \end{pmatrix}_{2\ell \times 2\ell}.$$

The matrix P is doubly stochastic, so that its stationary state is given by the uniform distribution $\pi = (1, 1, \cdots, 1)/2\ell$ for all parameters (p_1, p_2). The average current J and affinity A take the form

$$J = \frac{1}{2\ell}(p_1 + p_2 - 1) \tag{6}$$

and

$$A = \ell \ln \frac{p_1 p_2}{(1-p_1)(1-p_2)}. \tag{7}$$

The system is at equilibrium when $J = A = 0$ (i.e., when $p_2 = 1 - p_1$).

The activities $Y_e = J_e^+ + J_e^-$ along the edges read $Y_1 = (p_1 - p_2 + 1)/2\ell$ and $Y_2 = (p_2 - p_1 + 1)/2\ell$ depending if the transition is odd or even, respectively. However, only one edge is independent due to the symmetry of the model and the constraint $Y_1 + Y_2 = 1/\ell$. Taking

$$Y = Y_1 = \frac{1}{2\ell}(p_1 - p_2 + 1) \tag{8}$$

as the independent activity leads to an effective force

$$X = \ell(X_1 - X_2) = \ell \ln \frac{p_1(1 - p_2)}{p_2(1 - p_1)}. \tag{9}$$

Using expressions (7) and (9), the model parameters can be expressed as

$$p_1 = \frac{e^{(A+X)/2\ell}}{1 + e^{(A+X)/2\ell}}, \qquad p_2 = \frac{e^{(A-X)/2\ell}}{1 + e^{(A-X)/2\ell}}. \tag{10}$$

The iso-affinity classes are obtained by fixing A and varying X while the dynamical equivalence classes are obtained by varying the affinity A at fixed value of X [27]. The equilibrium manifold $A = 0$ is given by the line $p_2 = 1 - p_1$ (i.e., reversible motors) and the dynamical class $X = 0$ by the line $p_1 = p_2$ in parameter space (i.e., spatially homogeneous motors).

Within these manifolds or equivalence classes, the response curves are well-defined (Fig. 1). In this system, the current and activity have the same functional form within their respective equivalence classes. The current response curves are anti-symmetric, satisfy a fluctuation theorem, and capture fluctuation at all orders (i.e., deriving $J_X(A)$ with respect to A generates the various cumulants for any value of the affinity) [27].
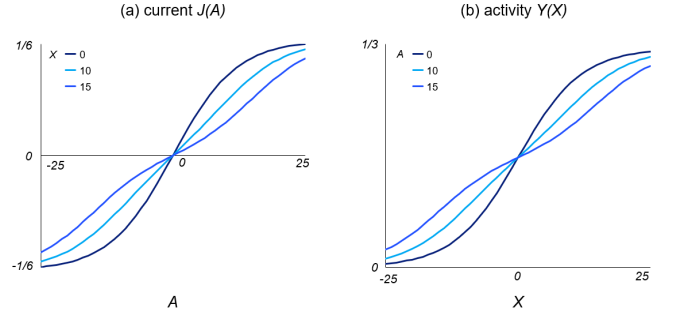

FIG. 1. **Current and activity response curves for the molecular motor** along equivalence classes. (a) Current response curves for different dynamical equivalence classes X. Each response curve is anti-symmetric and invariant under the transformation $X \to -X$ (not shown). (b) Activity response curves for different equivalence classes A. Each response curve is anti-symmetric (after translation) and invariant under the transformation $A \to -A$. In this system, the current and activity response curves have the same functional form within their respective (dynamical and iso-affinity) equivalence classes.

The activity response curves are antisymmetric (after translation to the origin) in the iso-affinity classes and are invariant under the transformation $A \to -A$ due to the time-reversal symmetry. As demonstrated in Appendix B, the activity satisfies a fluctuation theorem and, similar to the current, the response curves encode information about its fluctuations [10, 27]. The generalization of these observations to an arbitrary Markov system will be explored elsewhere.

The symmatrized KL divergence between two models $P = (p_1, p_2)$ and $G = (g_1, g_2)$ reads

$$\begin{aligned} 2\,D_{sKL} &= (p_1 - g_1)\ln\frac{p_1}{g_1} + (p_2 - g_2)\ln\frac{p_2}{g_2} \\ &+ (g_1 - p_1)\ln\frac{1-p_1}{1-g_1} + (g_2 - p_2)\ln\frac{1-p_2}{1-g_2}. \end{aligned}$$

Inserting the parametrization (10) into this expression leads to

$$\begin{aligned} D_{sKL}(P\|G) &= \frac{1}{2}(A_P - A_G)(J_P - J_G) \\ &+ \frac{1}{2}(X_P - X_G)(Y_P - Y_G). \end{aligned}$$

As expected from our general result, the divergence is expressed in terms of the system's current and affinity on the one hand, and the activity and kinetic force on the other hand.

As a result, the four embedding coordinates take the form

$$S_\alpha^\pm = \frac{1}{4}(A \pm J), \qquad S_e^\pm = \frac{1}{4}(X \pm Y).$$

In these coordinates, the molecular motor models form a two-dimensional manifold (Fig. 2) satisfying the Minkowski structure (5).
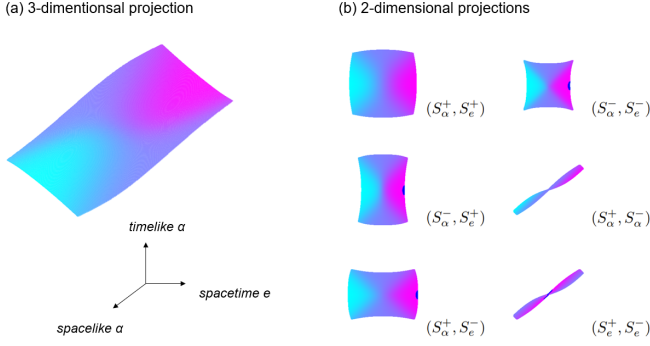
(a) 3-dimentionsal projection
(b) 2-dimensional projections

timelike α

spacetime e

spacelike α

(S_α^+, S_e^+) (S_α^-, S_e^-)

(S_α^-, S_e^+) (S_α^+, S_α^-)

(S_α^+, S_e^-) (S_e^+, S_e^-)

FIG. 2. **Model manifold for the molecular motor**. The molecular model manifold is embedded into $2 + 2$ dimensions. (a) A three-dimensional projection of the manifold, which is colored based on the current J. (b) The different two-dimensional projections of the manifold. The spacelike coordinates are denoted as S^+ and the timelike by S^-. For visual clarity, the embedding coordinates are scaled as $S_\alpha^\pm = (A/\lambda \pm \lambda J)/4$ and $S_e^\pm = (X/\lambda \pm \lambda Y)/4$ with $\lambda = L$. All 2-d projections have the same scale.

The embedding coordinates have similar shapes due to the similarity of the functional forms of $J_X(A)$ and $Y_A(X)$ (Fig. 1). Note that the number of embedding coordinates is independent of the size ℓ of the motor.

The entropy production is obtained as the divergence from the equilibrium component $E = P(X, 0) = P^{(e)}$ [23]:

$$\Delta_i S = J \times A = 2\, D_{sKL}\left(P||E\right) .$$

Similarly, the entropy production is also measured as the divergence with respect to $P^{(m)} = (P + P^*)/2 = (1/2)P(p_1 - p_2 + 1, p_2 - p_1 + 1)$ [23]. In that case $Y_P = Y_{P^{(m)}}$ even if $X_P \neq X_{P^{(m)}}$, so that $\Delta_i S = 2D_{sKL}(P||P^{(m)})$.

V. SUMMARY AND OUTLOOK

This work brings together thermodynamic and information geometric concepts, showing that thermodynamic quantities emerge naturally from the Minkoswki structure induced by the symmetrized KL divergence. While other divergences could be used, the symmetrized KL divergence bypasses the curse of dimensionality and provides the lowest embedding dimension, at least for exponential families of probability distributions [14, 28].

The embedding coordinates structure the space of Markov models in terms of equilibrium and nonequilibrium (i.e. symmetric and antisymmetric) components. The equilibrium coordinates are expressed in terms of the system's activities and kinetic forces while the nonequilibrium coordinates coincide with the dynamical equivalence classes and are expressed in terms of the system's currents and affinities. The symmetrized Kullback-Leibler divergence thus measures the difference in temporal and spatial structures between models.

This framework provides a systematic way to analyze the space of Markov models and to gain insights into the behavior and design of mesocopic devices. For example, the Minkowski embedding allows to explore a system's response in the directions 'orthogonal' to the dynamical equivalence classes, where additional symmetries are expected to appear. The embedding can be used to determine the minimum parameters needed to describe model data or to identify the governing parameters for model prediction and coarse graining [4, 28]. The space-time structure could also help untangle important phenomena such as dynamical or nonequilibrium phase transitions.

APPENDIX A: DERIVATION OF THE EMBEDDING COORDINATES

The first step to obtain Eq. (3) is to calculate the log ratios $\ln P_{ij}/G_{ij}$ that appear in Eq. (2). Using the thermodynamic decomposition (1) with $P = s[E \circ Z]$ and $G = s[E' \circ Z']$, the log ratios take the form

$$\ln \frac{P_{ij}}{G_{ij}} = \ln \frac{\rho'}{\rho} + \ln \left(\frac{\alpha_j'}{\alpha_i'} \frac{\alpha_i}{\alpha_j} \right) + \ln \frac{Z_{ij}}{Z_{ij}'} + \ln \frac{E_{ij}}{E_{ij}'} . \quad (11)$$

The first term $\ln \rho'/\rho$ vanishes when inserted into expression (2) since $\sum \pi_i P_{ij} = \sum \nu_i G_{ij} = 1$. The second term vanishes as well when averaged over a stochastic dynamics (see for example Lemma 4.3 (iii) in ref. [16]). The third term in Eq. (11) reads

$$(1/2) \sum_\alpha (A_\alpha - A_\alpha')(J_\alpha - J_\alpha') \quad (12)$$

when inserted into (2), where I used that $\ln Z_{ij} = \pm A_\alpha/2$ if the transition $i \to j$ corresponds to α in the positive (negative) direction, and 0 otherwise.

To calculate the last term $\ln E_{ij}/E_{ij}'$, remember that $E_{ij} = (1/\lambda)(\gamma_i/\gamma_j)\sqrt{P_{ij}P_{ji}}$ where λ and γ are the Perron eigenvalue and eigenvector of $\sqrt{P_{ij}P_{ji}}$, and similarly for E'. Here also the terms $\ln \lambda'/\lambda$ and $\ln(\gamma_j'\gamma_i/\gamma_i'\gamma_j)$ will vanish when averaged over $\sum \pi_i P_{ij} - \nu_i G_{ij}$. The remaining factor then becomes

$$(1/2) \sum_e (X_e - X_e')(Y_e - Y_e') , \quad (13)$$

where the sum runs over the $E + S$ edges and self-transitions $e = i \longleftrightarrow j$, $Y_e = J_e^+ + J_e^-$ is the average activity (sum of forward and backward currents) along an edge, and $X_e = \ln P_{ij}P_{ji}$. Note that only $E + S - 1$ factors Y_e are independent since $\sum_e Y_e = 1$. Summing the different terms gives the decomposition (3).

Finally, to obtain the embedding coordinates (4), each term in expression (12) can be written as [14]

$$(1/2)(A_\alpha - A_\alpha')(J_\alpha - J_\alpha') = (\Delta S_\alpha^+)^2 - (\Delta S_\alpha^-)^2$$

with the two coordinates

$$S_\alpha^\pm = (1/4)(A_\alpha \pm J_\alpha).$$

The same factorization applies to the terms $(X_e - X_e')(Y_e - Y_e')$ in Eq. (13). $\square$

APPENDIX B: FLUCTUATION THEOREM FOR THE MOLECULAR MOTOR ACTIVITY

In this section I show that the activity (8) of the molecular motor model satisfies a fluctuation theorem similar to the one for the currents (analytic expressions for the current fluctuations of the molecular motor are given in Ref. [27]).

In a given realization of the Markov chain, the activity will fluctuate as $y(n) = 1$ if the transition $i_{n-1} \to i_n$ matches one of the edges $i \longleftrightarrow i+1$ in any direction and with i odd (here denoted as an 'odd edge'), and 0 otherwise. The fluctuations of the activity are captured by the generating function

$$q(\lambda) = \lim_{n\to\infty} -\frac{1}{n} \left\langle e^{-\lambda \sum_n y(n)} \right\rangle_P.$$

The mean activity and its fluctuations are obtained by successive derivations of q with respect to λ. The generating function q is in turn obtained as

$$q(\lambda) = -\ln \rho[P \circ G(\lambda)],$$

where ρ denotes the largest eigenvalue of $P \circ G$ and

$$G_{ij}(\lambda) \equiv \begin{cases} \exp(-\lambda/\ell) & \text{if } i \to j \text{ is an odd edge,} \\ 1 & \text{otherwise}. \end{cases}$$

However, the activity y and its generating function $q(\lambda)$ do not display any symmetry. Rather, the *centered* activity

$$\bar{y} = y - 1/2\ell$$

such that $\langle \bar{y} \rangle (X = 0) = 0$ satisfies a fluctuation theorem.

The fluctuation theorem for the centered activity $\bar{y}$ can be demonstrated by calculating its generating function explicitly:

$$\bar{q}(\lambda) = -\frac{1}{2}\ln\left[\left(p_1 + (1-p_1)e^{\lambda/\ell}\right)\left(p_2 + (1-p_2)e^{-\lambda/\ell}\right)\right]$$

which satisfies the fluctuation theorem

$$\bar{q}(\lambda) = \bar{q}(X - \lambda).$$

The kinetic force X plays the same role as the affinity A in the current fluctuation theorem. Note that generating function of $\bar{y}$ and y are related as $\bar{q}(\lambda) = q(\lambda) - \lambda/2\ell$.

Similar to the current fluctuations within dynamical equivalence classes, the activity fluctuations within iso-affinity classes display additional symmetries beyond the fluctuation theorem. Expressing $\bar{q}$ in terms of the kinetic force and affinity of P,

$$\bar{q}(\lambda) = -\frac{1}{2}\ln\frac{\left(e^{(A-X)/2\ell}+e^{-\lambda/\ell}\right)\left(e^{(A+X)/2\ell}+e^{\lambda/\ell}\right)}{\left(e^{(A-X)/2\ell}+1\right)\left(e^{(A+X)2\ell}+1\right)},$$

shows that two dynamics X and X' within an iso-affinity class share the same generating functions modulo the shifts $\lambda \to \lambda + (X' - X)/2$ and $q' = q + (\bar{q}'(0) - \bar{q}(0))$. This shared functional form allows to obtain the activity fluctuations at all orders and for any value of the affinity A by deriving the activity response curve [10].

The activity fluctuation theorem and the role of iso-affinity classes for a general system will be explored elsewhere.

[1] T. L. Hill, *Free Energy Transduction and Biochemical Cycle Kinetics* (Dover, 2005).
[2] D. Andrieux, *Revealing hidden structures and symmetries in nonequilibrium transport*, arXiv:2401.14496 (2024).
[3] RN Gutenkun, JJ Waterfall, FP Casey, et al., *Universally sloppy parameter sensitivities in systems biology models*, PLoS Comput Biol 3: e189 (2007).
[4] B. B. Machta, R. Chachra, M. K. Transtrum, J. P. Sethna, *Parameter Space Compression Underlies Emergent Theories and Predictive Models*, Science **342**, 604 (2013).
[5] G. Falasco and M. Esposito, *Macroscopic Stochastic Thermodynamics*, arXiv:2307.12406 (2023).
[6] T. Aslyamov and M. Esposito, *Nonequilibrium Response for Markov Jump Processes: Exact Results and Tight Bounds*, Phys. Rev. Lett. **132**, 037101 (2024).
[7] D. Sivak and G. E. Crooks, *Thermodynamic metrics and optimal paths*, Phys. Rev. Lett. **108**, 190602 (2012).
[8] P. R. Zulkowski, D. A. Sivak, G. E. Crooks, and M. R. DeWeese, *The geometry of thermodynamic control*, Phys. Rev. E. **86**, 0141148 (2012).
[9] D. Andrieux, *Equivalence classes for large deviations*, arXiv:1208.5699 (2012).
[10] D. Andrieux, *Fully symmetric nonequilibrium response of stochastic systems*, arXiv:2205.10784 (2022).
[11] Shun-ichi Amari, *Information Geometry and Its Applications* (Springer, 2016).
[12] H. Nagaoka, *The exponential family of Markov chains and its information geometry*, The proceedings of the Symposium on Information Theory and Its Applications **28**, 601 (2005). Also available on arXiv:1701.06119.
[13] K. Quinn et al., *Visualizing probabilistic models and data with Intensive Principal Component Analysis*, Proc. Nat. Acad. Sci. **116**, 13762 (2019).
[14] H. K. Teoh et al., *Visualizing probabilistic models in Minkowski space with intensive symmetrized Kullback-

Leibler embedding, Phys. Rev. Res. **2**, 033221 (2020).

[15] J. Schnakenberg, *Network theory of microscopic and macroscopic behavior of master equation systems*, Rev. Mod. Phys **48**, 571 (1976).

[16] G. Wolfer and S. Watanabe, *Information Geometry of Reversible Markov Chains*, Information Geometry **4**, 393 (2021).

[17] S. Alpern, *Rotational representations of stochastic matrices*, The Annals of Probability **11**, 789 (1983).

[18] S. Kalpazidou, *Cycle Representations of Markov Processes* (Springer, 2006).

[19] D. Andrieux, *Nonequilibrium large deviations are determined by equilibrium dynamics*, arXiv:1212.1807 (2012).

[20] Two dynamics P and Q belong to the same class if there exists a scalar $\rho \geq 0$ such that: $(P \circ P^T)^{(1/2)} = \rho \, (Q \circ Q^T)^{(1/2)}$.

[21] While $D_{sKL}(P||G)$ is positive, symmetric and vanishes when $P = G$, in general it doesn't define a distance since the triangle inequality is not always respected.

[22] The role of the symmetric component in nonequilibrium response was highlighted by C. Maes and colleagues, see e.g. C. Maes and M. H. van Wieren, *Time-symmetric fluctuations in nonequilibrium systems*, Phys. Rev. Lett. **96**, 240601 (2006).

[23] D. Andrieux, *Irreversibility as divergence from equilibrium*, arXiv:2404.01978 (2024).

[24] P. Gaspard, *Time-reversed dynamical entropy and irreversibility in Markovian random processe*, J. Stat. Phys. **117**, 599 (2004).

[25] In analogy with the entropy production, the quantity $D_{sKL}(P||R) = (1/2) \sum_e X_e (Y_e - Y'_e) \geq 0$, where $R = s[T \circ Z(\boldsymbol{A})]$ with $\boldsymbol{A}$ the affinities of P and T its adjacency matrix, can be interpreted as measuring the asymmetry or 'inhomogeneity' in the graph's dynamics. Its properties remain to be explored.

[26] D. Andrieux and P. Gaspard, *Fluctuation theorems and the nonequilibrium thermodynamics of molecular motors*, Phys. Rev. E **74**, 011906 (2006).

[27] D. Andrieux, *Making sense of nonequilibrium current fluctuations: A molecular motor example*, arXiv:2306.01445 (2023).

[28] K. N. Quinn, M. C. Abbott, M. K. Transtrum, B. B. Machta and J. P. Sethna, *Information geometry for multiparameter models: new perspectives on the origin of simplicity*, Rep. Prog. Phys. **86**, 035901 (2023).